

Chapter 1

Fluid Flows

Flowing fluids are ubiquitous in Nature, from large scale atmospheric winds and oceanic currents to the circulation of blood or flow around microorganisms swimming in a liquid media. Fluid motion is also important in industrial processing and affects the motion of vehicles (cars, aircrafts etc.). In this chapter we briefly review the basic concepts and fundamental laws describing the motion of fluids. More details can be found in fluid dynamics textbooks (see, e.g. Batchelor (1967), Lamb (1932), Landau and Lifschitz (1959), Tritton (1988)).

In most cases one is interested in fluid flows at scales that are much larger than the distance between the molecules. The value of the molecular mean free path in air at room temperature and 1 atm of pressure is $\lambda = 6.7 \times 10^{-8}$ m and in water $\lambda = 2.5 \times 10^{-10}$ m. When the Knudsen number – defined as the ratio of the molecular mean-free-path to a characteristic length scale of the flow (e.g. the size of the smallest eddies) – is small, the fluid can be described as a continuous medium in motion. In this continuum approximation the flow can be characterized by the velocity field $\mathbf{v}(\mathbf{x}, t)$ representing the instantaneous velocity of infinitesimal fluid elements at time t and at position \mathbf{x} . Fluid elements represent small volumes of fluid that are much smaller than the smallest characteristic scale of the flow, but sufficiently large to contain a large number of molecules so that a well defined local velocity exists and molecular fluctuations can be neglected.

1.1 Conservation laws

The equations of fluid motion can be derived from the physical principles of conservation of mass, momentum and energy. The standard form of such conservation equations is

$$\frac{\partial A}{\partial t} + \nabla \cdot \mathbf{J} = S(\mathbf{x}, t) . \quad (1.1)$$

$A(\mathbf{x}, t)$ is the density of the quantity which is conserved, $\mathbf{J}(\mathbf{x}, t)$ is the flux, i.e. the amount of that quantity crossing the unit surface at location \mathbf{x} per unit of time. $S(\mathbf{x}, t)$ is the production (or consumption) rate of the quantity A per unit of volume at location \mathbf{x} . When $S = 0$, the balance between the terms in the left-hand-side indicates that the quantity A changes locally just because it is moving from place to place, so that it is globally conserved.

The conservation of the mass of a fluid in a velocity field $\mathbf{v}(\mathbf{x}, t)$ is expressed by Eq. (1.1) for the fluid density (mass per unit of volume) field $\rho(\mathbf{x}, t)$, with $S = 0$. The only process moving the fluid mass is transport by the velocity \mathbf{v} , giving the advective flux $\mathbf{J} = \rho\mathbf{v}$. Thus, Eq. (1.1) becomes the continuity equation

$$\frac{\partial \rho}{\partial t} + \nabla \cdot (\rho\mathbf{v}) = 0 . \quad (1.2)$$

The second term can be written as a sum of two components: $\mathbf{v} \cdot \nabla \rho$ that represents changes in the local density due to the flow bringing-in fluid of different density from elsewhere, and $\rho \nabla \cdot \mathbf{v}$ representing compression or expansion of the fluid volume when the velocity field is convergent ($\nabla \cdot \mathbf{v} < 0$) or divergent ($\nabla \cdot \mathbf{v} > 0$).

Under normal conditions most fluids are not compressed much in a flow. In general, if the typical flow velocity (U) is much smaller than the speed of sound (c) in the medium ($c_{air} \approx 340$ m/s, $c_{water} \approx 1500$ m/s), i.e. the Mach number, $\text{Ma} \equiv U/c$, is small, then the fluid is essentially incompressible. In this case the velocity field is a divergence-free (solenoidal) vector field

$$\nabla \cdot \mathbf{v} = 0 , \quad (1.3)$$

implying that the fluid density at a fixed location can only change due to transport from other fluid regions of different density.

The rate of change of a physical field $f(\mathbf{x}, t)$ along the trajectory of a fluid element, $\mathbf{r}(t)$, is obtained by differentiating $f[\mathbf{x} = \mathbf{r}(t), t]$ as

$$\frac{Df}{Dt} = \frac{\partial f}{\partial t} + \sum_i \frac{\partial f}{\partial x_i} \frac{dx_i}{dt} = \frac{\partial f}{\partial t} + (\mathbf{v} \cdot \nabla) f, \quad (1.4)$$

where the two components represent the rate of change in time at a fixed position and the change due to the motion of the fluid, respectively. The operator

$$\frac{D}{Dt} = \frac{\partial}{\partial t} + \mathbf{v} \cdot \nabla \quad (1.5)$$

is called the Lagrangian or material derivative. Thus, for an incompressible flow the continuity equation states that the Lagrangian derivative of the density is zero, $D\rho/Dt = 0$, meaning that the density is conserved along the path of the fluid elements. If initially the density is uniform in space then an incompressible flow maintains this uniform density.

The basic equation for the fluid velocity results from the conservation of momentum and can be obtained by applying Newton's law to a fluid element

$$\rho \frac{D\mathbf{v}}{Dt} = \mathcal{F} + \nabla \cdot \boldsymbol{\sigma}. \quad (1.6)$$

Acceleration of the fluid elements is due to two types of forces, body forces (per unit of volume), \mathcal{F} , acting within the whole fluid element volume (e.g. gravitational or electromagnetic forces) and forces acting on the surface of the small fluid element representing interaction with the rest of the fluid. The surface forces per unit of volume can be written as the divergence of a stress tensor $\boldsymbol{\sigma}$.

The stress tensor can be expressed as the sum of an isotropic diagonal part, a normal stress described by a scalar pressure p , and a deviatoric component or shear stress that appears as a result of internal friction between fluid layers moving relative to each other. In the simplest case of an incompressible Newtonian fluid the stress tensor is of the form

$$\boldsymbol{\sigma} = -p\mathbf{I} + \mu(\nabla\mathbf{v} + \nabla\mathbf{v}^T), \quad (1.7)$$

where the shear stress is assumed to be proportional to the strain tensor that describes the infinitesimal deformation rates of the fluid.

The coefficient μ is the dynamic viscosity, a fluid property that characterizes the resistance of the fluid to shearing forces and $(\nabla \mathbf{v})_{ij} = \partial v_i / \partial x_j$ is the velocity gradient tensor. Using this form of the stress tensor one obtains the Navier-Stokes equation

$$\frac{\partial \mathbf{v}}{\partial t} + \mathbf{v} \cdot \nabla \mathbf{v} = -\frac{1}{\rho} \nabla p + \nu \nabla^2 \mathbf{v} + \mathcal{F}, \quad (1.8)$$

where $\nu = \mu/\rho$ is the kinematic viscosity. Typical values are $\nu_{air} = 1.5 \times 10^{-5} \text{ m}^2/\text{s}$ and $\nu_{water} = 10^{-6} \text{ m}^2/\text{s}$. Thus the velocity at a point fixed in space changes due to inertia, i.e. advection of the velocity field by itself, pressure differences, internal friction and body forces. The equation needs to be supplemented with boundary conditions expressing that there is no flow through the boundary of the domain, and the “no-slip” condition, i.e. the fluid velocity at a solid boundary should be equal to that of the boundary. There are some special cases (e.g. in large-scale ocean models) where the no-slip condition is relaxed to allow for unrestricted fluid motion along the boundary. For ideal inviscid fluids ($\nu = 0$) the term representing viscous dissipation is dropped and the corresponding equation is called the Euler equation.

The momentum equation (1.8) together with the additional constraint of incompressibility (1.3) fully define the motion of an incompressible fluid. They form a system of four scalar equations for four unknown functions: the three components of the velocity field and the pressure field. Note that there is no evolution equation for the pressure field, which is given implicitly through the incompressibility condition. This somewhat complicates the analysis and numerical solution of the Navier-Stokes equation.

One way to eliminate the pressure from the Navier-Stokes equation is by transforming it into an equation for the vorticity field defined as the curl of the velocity field, $\boldsymbol{\omega} = \nabla \times \mathbf{v}$, that characterizes the distribution and direction of the rotational motion in the flow. By taking the curl of both sides of (1.8) and using the vector identity $(\mathbf{a} \cdot \nabla) \mathbf{a} = (1/2) \nabla |\mathbf{a}|^2 + (\nabla \times \mathbf{a}) \times \mathbf{a}$ and that for any scalar field ψ , $\nabla \times \nabla \psi = 0$ one obtains

$$\frac{\partial \boldsymbol{\omega}}{\partial t} = \nabla \times (\mathbf{v} \times \boldsymbol{\omega}) + \nu \nabla^2 \boldsymbol{\omega} + \nabla \times \mathcal{F}. \quad (1.9)$$

The nonlinear term can be further expressed as

$$\nabla \times (\mathbf{v} \times \boldsymbol{\omega}) = (\boldsymbol{\omega} \cdot \nabla) \mathbf{v} - (\mathbf{v} \cdot \nabla) \boldsymbol{\omega} + \mathbf{v}(\nabla \cdot \boldsymbol{\omega}) - \boldsymbol{\omega}(\nabla \cdot \mathbf{v}), \quad (1.10)$$

where the last two terms vanish because of $\nabla \cdot \boldsymbol{\omega} = \nabla \cdot (\nabla \times \mathbf{v}) = 0$ and incompressibility, $\nabla \cdot \mathbf{v} = 0$. Thus the dynamics of the vorticity field is described by the equation

$$\frac{\partial \boldsymbol{\omega}}{\partial t} + \mathbf{v} \cdot \nabla \boldsymbol{\omega} = \boldsymbol{\omega} \cdot \nabla \mathbf{v} + \nu \nabla^2 \boldsymbol{\omega} + \nabla \times \mathcal{F}. \quad (1.11)$$

This shows how the vorticity of a fluid is affected by the forcing and by the diffusion of vorticity. In addition, the first term on the right-hand-side representing “vortex stretching” also affects the vorticity field and the intensification of vorticity by the stretching of vortex tubes allows the transfer of vorticity and energy from large to smaller scales.

From the energetic point of view the work of the external forces produces fluid motion with a certain kinetic energy that is transformed into heat by internal friction. The energy balance can be obtained by multiplying the Navier-Stokes equation (1.8) by \mathbf{v} and integrating over the whole domain (an operation denoted by brackets $\langle \dots \rangle$). The contribution of the advective and pressure terms vanish for periodic or no-slip boundary conditions and we obtain

$$\frac{dE}{dt} \equiv \frac{1}{2} \frac{d\langle v^2 \rangle}{dt} = \langle \mathbf{v} \cdot \mathcal{F} \rangle - \nu \langle |\boldsymbol{\omega}|^2 \rangle, \quad (1.12)$$

where the mean square vorticity $\langle |\boldsymbol{\omega}|^2 \rangle$ is called the enstrophy. The second term on the right-hand-side is always negative. Thus in the absence of forcing the kinetic energy decreases monotonously due to viscous effects. In a forced stationary state the total energy is constant and there is a balance between the injection rate and the dissipation rate, which are the two terms in the right-hand-side of (1.12).

1.2 Laminar and turbulent flows

Depending on the forcing, boundary conditions and parameters, the Navier-Stokes equations describe a great variety of flows ranging from

time-independent laminar flows with a simple structure to highly complex swirling turbulent flows. It was first observed by O. Reynolds that the complexity of the flow depends on a non-dimensional parameter – named after him as the Reynolds number – defined as the typical magnitude of the ratio of the terms representing inertia and viscosity in the momentum equation (1.8):

$$\text{Re} = \frac{U(U/L)}{\nu U/L^2} = \frac{UL}{\nu}, \quad (1.13)$$

where L and U are characteristic length and velocity scales. Introducing the non-dimensional quantities $\mathbf{v}' = \mathbf{v}/U$, $t' = tU/L$, $\mathbf{x}' = \mathbf{x}/L$, $p' = p/(\rho U^2)$, $\mathcal{F}' = \mathcal{F}L/U^2$ (and dropping the primes) we obtain the non-dimensional form of the Navier-Stokes equation as

$$\frac{\partial \mathbf{v}}{\partial t} + \mathbf{v} \cdot \nabla \mathbf{v} = -\nabla p + \frac{1}{\text{Re}} \nabla^2 \mathbf{v} + \mathcal{F}, \quad (1.14)$$

Reynolds performed experiments using a transparent tube with a fine streak of dye injected into the flow for visualization (Reynolds, 1883). For low Re (i.e. small velocity, thin tube or high viscosity) the streak of dye was straight indicating a simple time-independent unidirectional flow parallel to the central axis of the tube. For large Re (e.g. obtained by applying a higher pressure difference that produces larger flow velocities) the dye streak broke up into an irregular fluctuating pattern as a consequence of the complex whirling fluid motion.

Similar laminar-turbulent transitions for increasing Re can be observed in range of different types of flows. One well known example is the flow in the wake of an obstacle (e.g. a cylinder with its axis perpendicular to the mean flow). For low Reynolds numbers the fluid simply passes around the cylinder. Then, at slightly higher Re a steady recirculation zone is created behind the cylinder breaking the symmetry between the upstream and downstream regions. When the Reynolds number is increased further the flow in the recirculation zone becomes time-dependent. First the velocity field oscillates periodically in time, producing the so called Kármán vortex street. Then the flow becomes aperiodic and for high Re it has a completely irregular fluctuating structure both in space and

time. Laminar-turbulent transition has also been studied extensively in fluid convection induced by a vertical temperature gradient producing an unstable density stratification (i.e. higher temperature at the lower boundary). Depending on the material properties of the fluid and the magnitude of the imposed temperature gradient there is a range of possible flow regimes including heat conduction with no flow, formation of a regular array of convection cells (rolls, hexagons etc.) with a time-independent velocity field, unsteady e.g. oscillating convection cells, and turbulent flow with an irregularly fluctuating structure in both space and time.

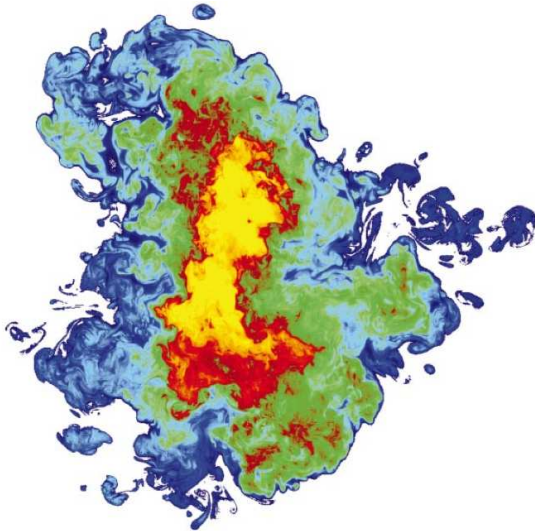


Figure 1.1: Complex multiscale flow structure shown by the concentration of a fluorescent dye in the cross section of a turbulent jet at $Re \sim 20000$ (experiment by Catrakis et al. (2002)).

Note that the laminar-turbulent transition is not a sharp transition that takes place at a fixed value of some parameters but rather there is a range of Reynolds numbers in which simpler flows became unstable and a sequence of transitions (bifurcations) gradually leads to the formation of more and more complex flow structures on a broad range of length and time scales that is characteristic to fully

developed turbulence (see Fig. 1.1). The details of the initial transitions and the corresponding values of Re depend on the type of flow considered, but typically it takes place around $Re \sim 10^3$.

Very large and very small Reynolds numbers both occur in real life flows. The flow around a bacteria of size about $1\mu\text{m}$ swimming in water at a typical speed of $15\mu\text{m/s}$ has a Reynolds number of about 10^{-5} , while for the airflow around a car ($L \approx 1\text{m}$) moving with a velocity $U = 100\text{ km/h}$, $Re \sim 10^6$. Large Reynolds number is also a characteristic feature of the large-scale geophysical flows with the well known consequence of the chaotic unpredictable nature of the daily weather.

When the Reynolds number is very small the inertial term can be neglected in the Navier-Stokes equation (1.14) and the velocity field is typically time-independent so that in the absence of external forces ($\mathcal{F} = 0$) the pressure differences are balanced by viscous forces

$$\nu \nabla^2 \mathbf{v} = \frac{1}{\rho} \nabla p. \quad (1.15)$$

This is the Stokes equation that has analytic solutions for certain types of simple laminar flows, for example the laminar flow in a straight channel known as Poiseuille flow (Fig. 1.2). Assuming that the flow is unidirectional along the x axis ($v_y = v_z = 0$) it follows from incompressibility that the velocity profile $v_x(y)$ is uniform along the channel. When a pressure difference δp is applied along a channel of length L and width d the Stokes equation reduces to

$$\nu v_x''(y) = \frac{1}{\rho} \delta p L. \quad (1.16)$$

The solution consistent with the no-slip boundary conditions $v_x(y = \pm d/2) = 0$ has a parabolic velocity profile (Fig. 1.2) of the form

$$v_x(y) = \frac{\delta p}{2\nu\rho L} \left(\frac{d^2}{4} - y^2 \right). \quad (1.17)$$

A similar solution can be obtained for the flow in a cylindrical pipe where y is replaced by the radial distance from the axis of the cylinder. There are a few other simple analytic solutions of the Stokes equation, e.g. for the flow around a sphere, etc. (Lamb, 1932).

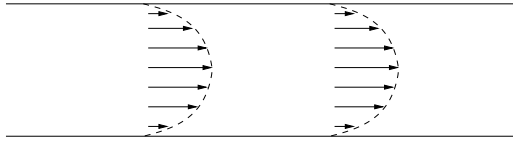


Figure 1.2: One of the simplest type of laminar flows: shear flow with a parabolic velocity profile in a straight channel.

Note that in fact the plane Poiseuille flow (1.17) is also an exact solution of the full Navier-Stokes equation. However, it was shown by linear stability analysis that this becomes unstable to small perturbations at a critical Reynolds number of 5772. In fact, the transition to turbulence is observed experimentally at even lower values of Re around 1000.

1.3 Turbulence

As already mentioned in the previous section, flows with a large Reynolds number have a strongly irregular, turbulent, character. Unfortunately it is not possible to obtain general analytic solutions of the Navier-Stokes equations for turbulent flows. Numerical solutions are also limited to moderate Reynolds numbers. This is due to the multiscale nature of the turbulent flows. As Re increases the range of length and time scales represented in the turbulent flow broadens and obtaining a good numerical approximation of the solution requires high resolution in space and time.

Another characteristic of turbulent flows is unpredictability, that is the high sensitivity of the solution to very small perturbations that are always present in real physical systems or numerical simulations. This unpredictability, also known as dynamical chaos, is a well known feature of much simpler low-dimensional nonlinear dynamical systems. Although in a strict mathematical sense a unique solution of the Navier-Stokes equation always exists for well-posed initial conditions (at least for large finite times), in practice the details of the forcing and boundary conditions are only known within some approximations and thus the solution in the turbulent regime repre-

sents only one of the possible typical realizations of the flow which are consistent with the initial and boundary conditions specified up to some finite precision. Although detailed information about a particular realization of a turbulent flow could be useful sometimes, for example in weather prediction, it is unnecessary in most situations. Therefore the general aim is to describe the statistical properties of the typical solutions such as mean values, typical deviations, probability densities etc. which are robust features of the flow and not affected by small perturbations.

An equation for the mean flow, defined as an average over many realizations of the turbulent velocity field, can be obtained (Reynolds, 1895) by decomposing the velocity and pressure fields into the sum of an ensemble-averaged and a fluctuating component:

$$\mathbf{v}(\mathbf{x}, t) = \mathbf{V}(\mathbf{x}, t) + \mathbf{v}'(\mathbf{x}, t), \quad p(\mathbf{x}, t) = P(\mathbf{x}, t) + p'(\mathbf{x}, t) \quad (1.18)$$

where $\mathbf{V} = \langle \mathbf{v} \rangle$ and $\mathbf{P} = \langle p \rangle$. The brackets $\langle \dots \rangle$ denote now ensemble averages. Note that in the turbulent flow regime the fluctuations are not small compared to the mean flow. From the continuity equation it follows, assuming an incompressible fluid, that the mean flow and the fluctuations are both divergence free. Substituting (1.18) into the Navier-Stokes equation and averaging gives

$$\frac{\partial V_i}{\partial t} + \sum_{j=1,2,3} V_j \frac{\partial V_i}{\partial x_j} = -\frac{1}{\rho} \frac{\partial P}{\partial x_i} + F_i + \nu \frac{\partial^2 V_i}{\partial x_i^2} - \sum_{j=1,2,3} \frac{\partial \langle v'_j v'_i \rangle}{\partial x_j}. \quad (1.19)$$

The averaging makes the fluctuations disappear from all the linear terms, but there is a contribution to the dynamics of the mean flow through the nonlinear term producing the last term on the right-hand side of (1.19). The symmetric tensor $\langle v'_i v'_j \rangle$ can be interpreted as an additional stress, known as the Reynolds stress, acting on the mean flow due to turbulence. The equation (1.19) for the mean flow is not closed. One can go further and obtain another equation for the correlations by subtracting (1.19) from the Navier-Stokes equation, but this will contain a term with third order correlations $\langle v'_i v'_j v'_k \rangle$, and so on for higher orders. This is known as the closure problem in turbulence, that is characteristic to nonlinear dynamical systems in general. The construction of approximate closure schemes for modelling turbulent flows has been an area of extensive research.

1.4 Kolmogorov's theory of turbulence

Richardson (1922) suggested the concept of an “energy cascade” for the description of turbulent flows. According to this the forcing injects energy into the flow and produces large eddies that became unstable and break up transferring their kinetic energy to somewhat smaller eddies. This “cascade” process generating smaller and smaller eddies continues until a smallest scale is reached at which the viscous forces dominate and the kinetic energy is converted into heat.

Significant progress towards a theoretical description of this cascade in homogeneous three-dimensional turbulent flows was made by Kolmogorov in a series of papers (Kolmogorov, 1941a,b). His theory is based on the assumption that at scales much smaller than the forcing scale (L) the turbulent flow has a universal statistically homogeneous and isotropic structure independent of the details of the forcing and of the large scale flow. Assuming statistical self-similarity of the velocity field the statistical properties of the flow describing the distribution of velocity fluctuations over different length scales can be expressed as universal functions of the energy dissipation rate and viscosity.

Kolmogorov further assumed that at sufficiently large Reynolds number and intermediate length scales, that are much smaller than the forcing scale but larger than the length scale where viscous dissipation becomes important, the statistics of the velocity field is independent of the viscosity and only depends on the overall energy dissipation rate. A consequence of this is that the energy dissipation rate per unit mass must tend to a non-zero constant in the limit of vanishing viscosity:

$$\lim_{\nu \rightarrow 0} \nu \langle (\nabla \times \mathbf{v})^2 \rangle = \epsilon > 0. \quad (1.20)$$

This appears to be in agreement with experimental observations. Since the viscosity term has the highest derivative in the Navier-Stokes equation the limit $\nu \rightarrow 0$ is singular and corresponds to divergent velocity gradients. This is an example of a dissipative anomaly in which the time-reversal symmetry, that is broken for the viscous flow, is not restored in the limit of vanishing viscosity.

Using the dissipation rate (ϵ) as the only relevant flow parameter in the $\nu \rightarrow 0$ limit, from dimensional considerations the typical fluctuations of the velocity field over a distance l and the corresponding characteristic timescales $\tau(l)$, usually interpreted as “eddy turnover time”, can be estimated as

$$\delta v(l) \sim (\epsilon l)^{1/3}, \quad \tau(l) = \frac{l}{v(l)} \sim \epsilon^{-1/3} l^{2/3}. \quad (1.21)$$

Thus, in the $\text{Re} \rightarrow \infty$ limit the turbulent velocity field is a rough non-differentiable function $\delta v(l) \sim l^{1/3}$ for $l \rightarrow 0$. This expression identifies the so-called Hölder exponent as $\alpha = 1/3$. It is easy to see that the energy transfer rate $\delta v(l)^2/\tau(l)$ is independent of the length scale l and applying the first of the above formulas to the integral scale (L) one can relate the energy dissipation rate to the large scale properties of the flow as $\epsilon \sim U^3/L$.

The results of this dimensional analysis are supported by an exact result obtained by Kolmogorov for the third-order longitudinal structure function. The structure functions are moments of velocity differences measured at a given distance. More specifically the structure function of order n , $S_n(l)$, is defined as

$$S_n(l) \equiv \langle [(\mathbf{v}(\mathbf{x} + \mathbf{l}) - \mathbf{v}(\mathbf{x})) \cdot \mathbf{l}/l]^n \rangle. \quad (1.22)$$

Brackets denote spatial or ensemble averages. Starting from the Navier-Stokes equation and assuming a statistically isotropic and homogeneous velocity field one can derive the Kármán-Howarth equation for the longitudinal structure functions as

$$\frac{\partial S_2}{\partial t} + \frac{1}{3l^4} \frac{\partial}{\partial l} (l^4 S_3) + \frac{4}{3} \epsilon = \frac{2\nu}{l^4} \frac{\partial}{\partial l} \left(l^4 \frac{\partial S_2}{\partial l} \right). \quad (1.23)$$

Taking the $\nu \rightarrow 0$ limit in a stationary state the third moment of the longitudinal velocity differences is obtained as

$$S_3(l) = -\frac{4}{5} \epsilon l. \quad (1.24)$$

Note that this is consistent with the scaling (1.21) based on the universality and self-similarity assumptions ($\delta v(l) = S_1(l)$).

Using the statistical self-similarity hypothesis this exact result can be generalized to the n th order structure functions as

$$S_n(l) = C_n \epsilon^{n/3} l^{n/3}, \quad (1.25)$$

where C_n are dimensionless constants.

Alternatively, the fluctuating velocity field can be characterized by the energy spectrum defined as the Fourier transform of the two-point velocity correlation integrated over a spherical shell of wavenumbers with magnitude k :

$$E(k) = \frac{1}{2(2\pi)^3} \int \left[\int \langle \mathbf{v}(\mathbf{x}) \cdot \mathbf{v}(\mathbf{x} + \mathbf{r}) \rangle e^{-i\mathbf{k}\mathbf{r}} d\mathbf{r} \right] \delta(|\mathbf{k}| - k) dk. \quad (1.26)$$

From Kolmogorov's hypotheses it follows that the energy spectrum at large Re has a form $E(k) = f(k, \epsilon)$ and dimensional analysis yields

$$E(k) = C_K \epsilon^{2/3} k^{-5/3} \quad (1.27)$$

where C_K is called the Kolmogorov constant that from experimental data is around $C_K \simeq 1.5$. The spectral exponent $\gamma = 5/3$ can also be obtained from the mathematical relationship between γ and the exponent of the second-order structure function $S_2 \sim l^{\zeta_2}$, as $\gamma = 1 + \zeta_2$.

For large, but finite Reynolds numbers the above scalings remain valid in the range of lengthscales where both the energy injection due to external forces and the viscous dissipation can be neglected. Viscous dissipation becomes important at the lengthscale where the eddy turnover time $\tau(l)$ is comparable to the characteristic time of diffusion of momentum l^2/ν . Alternatively one can define a scale-dependent effective Reynolds number that measures the ratio of the inertial and viscous terms for eddies of size l as $\text{Re}(l) = \delta v(l)l/\nu$. For turbulent flows with $\text{Re} = \text{Re}(L) \gg 1$ there is a range of scales where viscous dissipation is negligible and the kinetic energy flows to smaller scales without any losses. The lengthscale η where this energy cascade ends is thus given by the condition

$$\text{Re}(\eta) = \frac{\delta v(\eta)\eta}{\nu} \simeq \mathcal{O}(1). \quad (1.28)$$

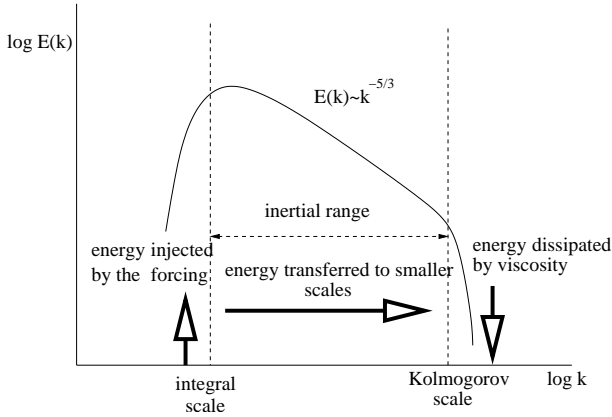


Figure 1.3: Schematic diagram of the kinetic energy spectrum of a turbulent flow.

Using (1.21) this gives

$$\eta \sim \left(\frac{\nu^3}{\epsilon}\right)^{\frac{1}{4}} \sim \left(\frac{L\nu^3}{U^3}\right)^{\frac{1}{4}} = \frac{L}{\text{Re}^{3/4}}. \quad (1.29)$$

This is the Kolmogorov scale that represents the size of the smallest flow structures in the turbulent velocity field. Thus, the range of validity of the scalings in (1.21) and (1.25) is given by the so called inertial range where $L \gg l \gg \eta$ (see Fig. 1.3). Note that the lengthscale ratio of the largest and smallest eddies increases with the Reynolds number as $\text{Re}^{3/4}$. Thus the number of gridpoints or Fourier modes needed to fully resolve a three-dimensional turbulent flow in a numerical simulation can be estimated as $(L/\eta)^3 \sim \text{Re}^{9/4}$ indicating that many of the naturally occurring highly turbulent flows are well beyond the reach of the capacity of current computers.

Experiments are in good agreement with the predicted $-5/3$ energy spectrum (1.27), but there are significant deviations from (1.25) for higher order structure functions with $n > 3$. They follow power laws $S_n(l) \sim l^{\zeta_n}$, but with scaling exponents $\zeta_n < n/3$ that do not satisfy the self-similarity hypotheses (Sreenivasan and Antonia, 1997). These deviations are due to the intermittent, strongly non-

homogeneous character of the velocity fluctuations, that cannot be described by a single constant value of the dissipation rate. Currently, there is no satisfactory theoretical description for the experimentally measured anomalous scaling exponents. Further information on Kolmogorov's theory, their corrections, and turbulent flows in general, can be found in books such as Batchelor (1953), Frisch (1995), Lesieur (1990), or Pope (2000).

1.5 Two-dimensional flows

Although strictly speaking there are no two-dimensional flows in nature there has been considerable research on turbulent flows in two spatial dimensions (see the reviews by Kraichnan and Montgomery (1980) or Tabeling (2002)). This has been partly motivated by the interest in geophysical flows that can be considered quasi-two-dimensional since stable density stratification and the Earth's rotation both restrict large scale motions to two-dimensional layers. Quasi-two-dimensional turbulent flows have also been studied in laboratory experiments with soap films, density stratification or using rotating tanks. Obviously, two-dimensional turbulence is also more accessible for high resolution numerical simulations.

It turns out that there are significant differences in some aspects of turbulence between three- and two-dimensional systems. As the vorticity vector points in the direction perpendicular to the plane of the flow $\boldsymbol{\omega} \perp \mathbf{v}$, fluid motion can be fully described by a scalar field $\omega(x, y)$. A consequence of two-dimensionality is that the vortex stretching term $\boldsymbol{\omega} \cdot \nabla \mathbf{v}$ vanishes in the vorticity equation (1.11) that becomes

$$\frac{\partial \omega}{\partial t} + \mathbf{v} \cdot \nabla \omega = \nu \nabla^2 \omega + |\nabla \times \mathcal{F}|. \quad (1.30)$$

Thus, in the absence of the forcing and viscous dissipation the vorticity is conserved along the trajectories of fluid elements. Equation (1.30) describes the evolution of the vorticity distribution in a given velocity field. However, ω and \mathbf{v} are obviously not independent of each other, but are two alternative representations of the instantaneous flow field. The velocity field is a vector, but it is subjected to the incompressibility condition. This constraint can be eliminated

in two-dimensional flows by introducing the scalar streamfunction $\psi(x, y, t)$ that defines the flow as

$$v_x = -\frac{\partial\psi}{\partial y}, \quad v_y = \frac{\partial\psi}{\partial x} \quad (1.31)$$

and automatically satisfies incompressibility. Taking the curl of the velocity field one obtains a relationship between the streamfunction and vorticity field as

$$\omega(x, y) = \frac{\partial^2\psi}{\partial x^2} + \frac{\partial^2\psi}{\partial y^2}. \quad (1.32)$$

Thus the dynamics can be described from (1.30) as the vorticity field advected by the flow defined by the streamfunction (1.31) while the new streamfunction at a later time can be obtained from the vorticity field by inverting (1.32). This second step is computationally expensive since it requires the solution of an elliptic equation in which the streamfunction at any given point depends on the whole distribution of vorticity.

In the case of a two-dimensional inviscid fluid with no forcing a special class of simple analytic solutions is a system of point vortices represented as a singular distribution of vorticity concentrated on a set of points

$$\omega(\mathbf{x}, t) = \sum_i \Gamma_i \delta(|\mathbf{x} - \mathbf{r}_i(t)|), \quad (1.33)$$

where Γ_i and \mathbf{r}_i are the strength and position of the i th vortex, respectively. The streamfunction for the velocity field generated by the point vortex system can be obtained from (1.32) as the Green's function of the Laplace equation

$$\psi(\mathbf{x}, t) = -\sum_i \frac{\Gamma_i}{2\pi} \log |\mathbf{x} - \mathbf{r}_i(t)| \quad (1.34)$$

and the velocity components of a single point vortex in polar coordinates with the origin at the vortex center are

$$v_r = 0, \quad v_\phi = \frac{\Gamma}{2\pi r}. \quad (1.35)$$

Since the vorticity is conserved within the fluid elements the equation of motion for the vortex centers in a system of point vortices is given by the advection equation $\dot{\mathbf{r}}_i = \mathbf{v}[\mathbf{x} = \mathbf{r}_i(t), t]$. Each point vortex is passively advected just like any other fluid element by the superposition of the velocity fields generated by all the other vortices (excluding self-interaction). Thus the equation of motion of a system of point vortices is given by

$$\dot{x}_i = -\frac{1}{2\pi} \sum_{j \neq i} \frac{\Gamma_j (y_i - y_j)}{r_{ij}^2}, \quad \dot{y}_i = \frac{1}{2\pi} \sum_{j \neq i} \frac{\Gamma_j (x_i - x_j)}{r_{ij}^2}, \quad (1.36)$$

where $r_{ij} = |\mathbf{r}_i - \mathbf{r}_j|$ is the distance between vortices i and j . This type of point vortex systems exhibit a great variety of flows (Aref, 1983) and have been used as model flows in theoretical studies of mixing.

More complex turbulent-flow solutions appear in the presence of forcing and non-zero viscosity. As mentioned earlier the vortex stretching mechanism for transferring energy to smaller scales does not operate in two-dimensional turbulent flows. In the absence of forcing and viscosity the vorticity is conserved along the trajectories, $D\omega/Dt = 0$. Thus vorticity can not diverge in the inviscid limit and the viscous energy dissipation rate $\nu \langle \omega^2 \rangle$ vanishes as $\nu \rightarrow 0$. Thus, from (1.12) the energy cannot be removed by viscosity at small scales in the $\nu \rightarrow 0$ limit. This rules out the possibility of the direct energy cascade to smaller scales as in three-dimensional turbulence. Kraichnan (1967) suggested that the energy injected into the flow by the forcing is transferred to larger scales resulting in an “inverse energy cascade”. In a finite system the energy is eventually dissipated by friction acting at the boundaries or by other large scale processes. In numerical simulations a stationary state can be established by introducing some sort of damping to prevent the accumulation of energy at the largest scales set by the size of the computational domain. Dimensional arguments imply that the energy spectrum for the inverse cascade range, i.e. between the largest scale and the forcing scale has the same form as in three dimensions: $E(k) = C' \epsilon^{2/3} k^{-5/3}$ and the predicted $k^{-5/3}$ power law has been verified in experiments and numerical simulations (Tabeling, 2002). The scaling of the structure functions follows $S_n(l) \sim l^{n/3}$ and in contrast with three-dimensional

turbulence the experimental data do not show significant deviations from this due to intermittency, in this large scale range.

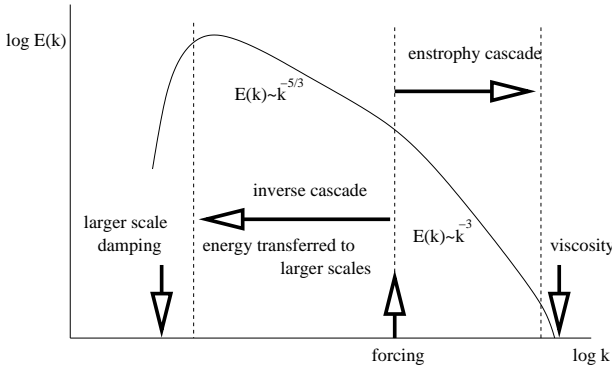


Figure 1.4: Schematics of the dual cascade energy spectrum in two-dimensional turbulence.

Batchelor (1969) and Kraichnan (1967) also proposed the existence of another cascade in two-dimensional flows that is associated with the transfer of the enstrophy to smaller scales through the formation of thin vorticity filaments due to the large scale strain generating strong vorticity gradients. The enstrophy cascade ends at a small length scale where enstrophy is dissipated by the diffusion of vorticity due to molecular viscosity. Assuming a constant flux of enstrophy gives an energy spectrum of the form $E(k) \sim \theta^{2/3} k^{-3}$ at scales below the forcing scale, where $\theta = \nu \langle (\nabla \omega)^2 \rangle$ is the enstrophy dissipation rate. Similarly to the energy dissipation rate in three-dimensional turbulence the enstrophy dissipation rate converges to a finite constant in the limit of vanishing viscosity. At finite viscosity the enstrophy cascade ends at the length scale $l_Z = \theta^{-1/6} \nu^{1/2}$.

Note that in contrast to the “rough” velocity field of three-dimensional turbulence, the k^{-3} spectrum implies an almost everywhere smooth velocity field at small scales such that $\delta v(l) \sim l$ (with logarithmic corrections). This also means that at scales below the forcing scale, within the enstrophy cascade range, the flow has a single characteristic timescale: $\tau(l) \sim l/\delta v(l) \approx \tau^*$, which is independent of the lengthscale l .

The theoretically predicted dual cascade with two power-law regimes in the kinetic energy spectrum (Fig. 1.4) has been reproduced in numerical simulations and confirmed by laboratory experiments. In some of the experiments spectra steeper than k^{-3} was observed in the enstrophy cascade range. This deviation can be related to the presence of additional damping at large scales, the so-called Ekman friction. Since the theoretical description of this regime is very similar to the problem of chemical decay in smooth flows we will return to this later in Chapter 6.